(4)

The Quantum Yield of NF(a) in NF$_2$ Photolysis

J. F. BOTT
Aerophysics Laboratory
Laboratory Operations
The Aerospace Corporation

4 November 1987

DTIC
ELECTE
DEC 2 3 1987
D
D

Prepared for

AIR FORCE WEAPONS LABORATORY
Kirtland Air Force Base, NM 87117

SPACE DIVISION
AIR FORCE SYSTEMS COMMAND
Los Angeles Air Force Station
P.O. Box 92960, Worldway Postal Center
Los Angeles, CA 90009-2960

87 12 14 066

REPORT DOCUMENTATION PAGE

1a. REPORT SECURITY CLASSIFICATION	1b. RESTRICTIVE MARKINGS

2a. SECURITY CLASSIFICATION AUTHORITY	3. DISTRIBUTION / AVAILABILITY OF REPORT
2b. DECLASSIFICATION / DOWNGRADING SCHEDULE	Approved for public release; distribution unlimited

4. PERFORMING ORGANIZATION REPORT NUMBER(S)	5. MONITORING ORGANIZATION REPORT NUMBER(S)
TR-0086A(2604)-1	SD TR-87-55

6a. NAME OF PERFORMING ORGANIZATION	6b. OFFICE SYMBOL (If applicable)	7a. NAME OF MONITORING ORGANIZATION
The Aerospace Corporation Laboratory Operations		Space Division

6c. ADDRESS (City, State, and ZIP Code)	7b. ADDRESS (City, State, and ZIP Code)
	Los Angeles Air Force Station Los Angeles, CA 90009-2960

8a. NAME OF FUNDING / SPONSORING ORGANIZATION	8b. OFFICE SYMBOL (If applicable)	9. PROCUREMENT INSTRUMENT IDENTIFICATION NUMBER

8c. ADDRESS (City, State, and ZIP Code)	10 SOURCE OF FUNDING NUMBERS			
	PROGRAM ELEMENT NO.	PROJECT NO.	TASK NO.	WORK UNIT ACCESSION NO.

11. TITLE (Include Security Classification)

The Quantum Yield of $NF_{(a)}$ in NF_2 Photolysis

12. PERSONAL AUTHOR(S) Bott, J. F.

13a. TYPE OF REPORT	13b. TIME COVERED FROM _____ TO _____	14. DATE OF REPORT (Year, Month, Day) 1987, November 4	15. PAGE COUNT 11

16. SUPPLEMENTARY NOTATION

17. COSATI CODES			18. SUBJECT TERMS (Continue on reverse if necessary and identify by block number)
FIELD	GROUP	SUB-GROUP	Branching fraction
			NF(a) fluorescence

19. ABSTRACT (Continue on reverse if necessary and identify by block number)

Koffend, Gardner, and Heidner performed experiments to determine the quantum yield of NF(a) in the photolysis of NF_2 at 249 nm and the rate coefficient for the combination of F atoms with NF_2 and Ar. Their data analysis was based on a value of 0.91 for the branching fraction of NF(a) produced in the $H+NF_2$ reaction. This report shows that the quantum yield can be determined independently of the branching fraction and that the value of the combination rate coefficient is directly proportional to the branching fraction. The fact that the photolysis quantum yield can be determined independently of the branching fraction is important because experiments for measuring the branching fraction can now be designed in which the initial NF(a) fluorescence serves as a calibration of the system for subsequent NF(a) measurements.

20. DISTRIBUTION / AVAILABILITY OF ABSTRACT ☐ UNCLASSIFIED/UNLIMITED ☐ SAME AS RPT ☐ DTIC USERS	21. ABSTRACT SECURITY CLASSIFICATION
22a. NAME OF RESPONSIBLE INDIVIDUAL	22b. TELEPHONE (Include Area Code) 22c OFFICE SYMBOL Unclassified

DD FORM 1473, 84 MAR 83 APR edition may be used until exhausted. SECURITY CLASSIFICATION OF THIS PAGE

All other editions are obsolete.

Introduction

Koffend et al. (Ref. 1) performed experiments to determine (1) the quantum yield of NF(a) production in the 249 nm photolysis of NF_2 and (2) the rate coefficient for the three-body combination of F atoms with NF_2 and Ar. They used a KrF laser to photolyze a small fraction of NF_2 in gas mixtures containing H_2 and argon and recorded the maximum NF(a) fluorescence. These data plotted versus the argon concentration (and also versus the H_2 concentration) allowed the rate coefficient for the combination of F atoms with NF_2 to be extracted with a simplified theoretical analysis. The quantum yield of NF(a) was calculated from NF(a) fluorescence measurements for photolyzed mixtures of NF_2 and argon using the measured detector sensitivity. The detector sensitivity for NF(a) fluorescence was calibrated by relating the detector signal obtained for a particular set of experimental conditions to the NF(a) density calculated with NEST, a kinetics code, for those conditions. The branching fraction for NF(a) production in the reaction

$$H + NF_2 \rightarrow NF(X,a,b) + HF$$

was assumed in the NEST calculations to have a value of 0.91, as determined by Malins and Setser (Ref. 2) and Cheah and Clyne (Ref. 3).

Therefore, the values of the photolysis quantum yield and the recombination rate coefficient were determined on the basis of an assumed large branching fraction. Whitefield and Hovis (Ref. 4) have reported chemical kinetic studies which suggest that the branching fraction is considerably less than 0.91. The purpose of this report is to show how the determinations of the above values depend on the assumed value of the branching fraction and to offer some evidence to support the large branching fraction.

Analysis and Discussion

The photolysis produces the radicals NF(X) + NF(a) and a quantity of F atoms equal to the sum of the radicals. Certain generalizations can be made about the fate of these radicals in a gas mixture for which

1

A-1

$[F] \ll [H_2] \ll [NF_2] \ll [Ar]$. The NF(X) radicals combine to produce F atoms. The F atoms react with H_2, yielding H atoms which then react with NF_2 according to the above reaction. NF(a) produced in the reaction increases to a maximum before finally decreasing at long times due to deactivation. At intermediate times F, NF(X), and H react away, leaving NF(a), H_2, NF_2, argon, and the NF_3 formed by the combination of NF_2 and F in collisions with argon. The deactivation of NF(a) is the slowest and, therefore, the rate limiting step toward final equilibration. The amount of NF_3 produced (and also the amount of H_2 consumed) will depend on the branching fraction and on the rate of the F atom combination with NF_2 relative to its rate of reaction with H_2. Figure 8 of Ref. 1 shows a time history of the NF(a) fluorescence. Only if the branching fraction were sufficiently small or the deactivation processes were faster would the NF(a) fluorescence not increase from its initial intensity. The ratio of the initial fluorescence intensity to the maximum intensity is of particular importance for the determination of the quantum yield.

Koffend et al. used a simplified four-reaction mechanism to describe the important processes in their experiments. They derived an approximate equation for the time dependence of NF(a) in the Appendix of Ref. 1, from which they obtained their Eq. 10 for the dependence of the maximum NF(a) fluorescence on the argon and H_2 densities. They performed two sets of experiments; in one set only the argon concentration was varied and in the other only the H_2 was varied (see Figs. 6 and 7 of Ref. 1). Using Eq. 10 they obtained a value for the recombination rate coefficient of $(1.0\pm0.3) \times 10^{-30}$ $cm^6/molecule^2sec$ from the data of Fig. 6 in which the argon was varied and $(1.1\pm0.2) \times 10^{-30}$ $cm^6/molecule^2sec$ from the data of Fig. 7 in which the H_2 was varied.

Their Eq. 10 was derived assuming the NF(a) branching fraction for the reaction of H with NF_2 to be equal to 1. However, a similar equation can be derived in which the branching fraction is included as the parameter B.

$$1/([NF(a)]-[NF(a)]_o) = \left(1 + \frac{k_3 \times [NF_2] \times [Ar]}{B \times k_2 \times [H_2]}\right)/([NF(X)]_o + [F]_o) \qquad (1)$$

2

$[NF(a)]_o$ is the initial NF(a) produced by the photolysis, $[NF(a)]$ is the maximum density achieved at intermediate times, k_3 is the recombination rate coefficient, and k_2 is the rate coefficient for the reaction of F with H_2. This equation is the same as Eq. 10 of Ref. 1 except that k_3 has been replaced with k_3/B and $[NF(a)]$ has been replaced with $([NF(a)] - [NF(a)]_o)$. When this equation is fitted to the data of Fig. 6 in Ref. 1 we obtain

$$k_3/B = 0.96 \times 10^{-30}/(1 - 1.29 \times Q) \qquad cm^6/molecule^2 sec \qquad (2)$$

where B is the branching fraction and Q is the quantum yield of NF(a). $[NF(a)]_o$, $[NF(X)]_o$, and $[F]_o$ can be related to each other with Q. Equation 1 does not predict a completely linear dependence of $1/[NF(a)]$ on the Ar concentration. However, the nonlinearity is smaller than the scatter of the data in Fig. 6. Equation 2 gives $k_3 = 1.0 \times 10^{-30}$ for B = 0.91 and Q = 0.10, in agreement with the value deduced in Ref. 1. An analysis of the data in Fig. 7 of Ref. 1 yields an expression in basic agreement with Eq. 2 but smaller by about 8%. As pointed out in Ref. 1, an absolute calibration of the intensity is not required since it occurs in both the slope and the intercept of the data and can be eliminated by taking their ratio. The uncertainty in the value of k_3/B includes the uncertainties of the intensity ratio (±10%), the concentrations of NF_2, H_2, and Ar, and the value of k_2 (±25%). With a contribution of 10% from the gas concentrations, we estimate the total RMS uncertainty of k_3/B to be ±40%.

Koffend et al. used the experimental data of their Fig. 8 and the results of a kinetics code calculation to calibrate the sensitivity of their detector for NF(a) fluorescence. This calibration allowed them to calculate the quantum yield of NF(a) from measurements of the NF(a) fluorescence in photolyzed NF_2/argon mixtures. However, the quantum yield, Q, can also be determined directly from Fig. 8 without an absolute calibration. Since $[NF(a)]_o = Q \times F_o$ and $[NF(X)]_o = (1-Q) \times [F]_o$, Eq. 1 can be rearranged to give

$$2/Q = \left(1 + \frac{k_3 \times [NF_2] \times [Ar]}{B \times k_2 \times [H_2]}\right) \times ([NF(a)]/[NF(a)]_o - 1) + 1 \qquad (3)$$

Therefore, the quantum yield, Q, depends only on the ratio of $[NF(a)]$ final to $[NF(a)]_o$ and the recombination parameter, k_3/B, which is given independently by Eq. 2.

3

Figure 8 of Ref. 1 shows the maximum NF(a) fluorescence to be 11 times the initial NF(a)$_o$ fluorescence. Only the ratio of the initial to the final-fluorescence and not the absolute values assigned to them in the figure is important. (The figure caption erroneously states that [NF(a)]$_o$ = 2.6E+12, however, it is plotted as 1.9E+12.) With the ratio of 11 and the initial concentrations of the gas mixture, we calculate a value of Q = 0.10. As noted in Ref. 1, the approximate analysis does not take into account the conversion of possibly 15% of the NF(a) to NF(b); taking it into account reduces the quantum yield to a value of 0.083. There is also a depletion of about 20% of the H$_2$ over the course of the reaction allowing slightly more recombination to NF$_3$ than our analysis takes into account. Taking this into account reduces the value of Q by 5% to a value of Q = 0.08±0.02. The uncertainty in the present value includes a ±10% uncertainty in the ratio of the final to the initial fluorescence intensity and the uncertainty in the parameter of $(k_3 \times [NF_2] \times [Ar])/(B \times k_2 \times [H_2])$. This latter parameter is determined essentially from the ratio of the slope to the intercept in Fig. 6 and then scaled to the appropriate Ar, NF$_2$, and H$_2$ conditions and should be no more uncertain than about 15%. The RMS value of these several uncertainties is about ±25%. The uncertainty could be reduced by analyzing data obtained at lower Ar pressures (or higher H$_2$ pressures) with smaller contributions of the recombination parameter. Also, a larger concentration of H$_2$ would decrease its percentage change during the reactions.

Figure 8 of Ref. 1 allows us to determine the quantum yield, Q, but it also allows us to estimate the branching fraction, B. The value of Q is determined from the ratio of the final to the initial fluorescence intensity while the value of B is determined from the risetime of the fluorescence. Koffend et al. show in their Fig. 8 a good fit of their theoretical calcula-tions (both the approximate model and the more complete NEST calculations in which B was assumed to be 0.91) to the experimental fluorescence profile. In Fig. 1 we show NF(a) profiles obtained numerically with the same four-reaction mechanism used by Koffend et al. to match their data of Fig. 8. In addition to the profile calculated with B = 0.91, we also show profiles calculated for values of B = 0.6 and 0.3. The assumed value of B has a big effect on the risetime of the fluorescence since it directly affects the production rate of NF(a). For the smaller values of the branching fraction, B, the chain has to run longer to convert the F and NF(X) radicals to NF(a) and NF$_3$ since both the

4

production rate of NF(a) and our value deduced for k_3, the recombination rate coefficient, depend directly on the value of B. For lower values of B, more of the H_2 is consumed so that the H_2 density drops somewhat during the course of the reactions; this slows the F + H_2 reaction in comparison to the combination of F and NF_2 and reduces the total yield of NF(a). If H_2 were in large excess and remained constant, the total yield of NF(a) would be independent of the value of B. The precision of the data and the good fit with the calculated profile (particularly the NEST calculations) in Fig. 8 probably preclude values of B as low as even 0.6. A precise error analysis is somewhat complicated, but a value of B = 0.9 (+0.1,−0.2) seems reasonable. It should be noted that the calculation of the NF(a) profile depends only weakly on the absolute concentrations. All of the equations for the four-reaction mechanism are linear except for the reaction of NF(X) with itself in which two F atoms are produced. This linearity reduces the dependence of the analysis on an absolute calibration of the detector sensitivity and the measurement of the photolysis laser fluence.

Koffend et al. compared their value for k_3 with other values in the literature. Their value seemed to be larger than one might estimate from the literature values reported for other temperatures and third bodies. A value of B much less than 0.91 would reconcile this discrepancy but would contradict the work of Refs. 2 and 3 as well as the analysis presented in this report.
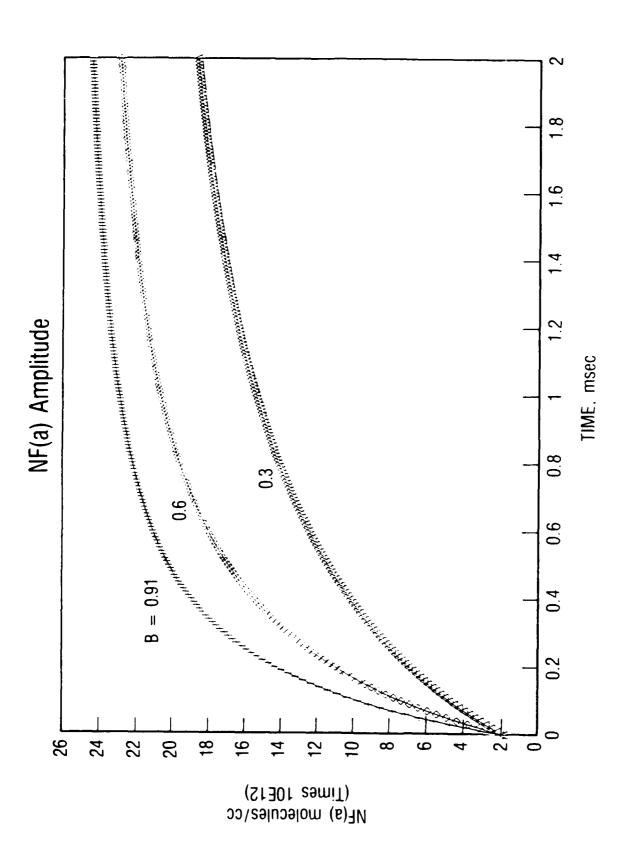
Our analysis does not change the results of Koffend et al. but rather confirms their value for the recombination coefficient, substantiates the value of the branching fraction, and yields a value of the quantum yield, 0.08±0.02 in substantial agreement with their value of 0.10±0.05. In fact, their "best" calibration factor of 2.13E+8 cc/molecule/lab unit combined with the peak signal of 18,000 lab units in their Fig. 2 gives an NF(a) peak density of 3.8E+12 molecules/cc. For the laser fluence of 8E+15 photons/cm^2, [NF_2] = 9.8E+15 molecules/cm^3, and an absorption cross-section of 6.8E-19/cm^2, one calculates a quantum yield of 0.072. This agreement supports the consistency of the two different approaches to the quantum yield determination.

The fact that the value of the quantum yield can be determined independently of the branching fraction is important. Experiments can now be designed such that the initial NF(a) fluorescence (or the final NF(a) fluorescence from a properly chosen mixture) serves as a calibration for subsequent NF(a) meas-

urements. Such a calibration will still require the absorption cross-section and measurements of the laser fluence and NF_2, if absolute concentrations are required.

REFERENCES

1. J. B. Koffend. C. E. Gardner, and R. F. Heidner, J. Chem. Phys. 83, 2904 (1985).

2. R. J. Malins and D. W. Setser, J. Phys. Chem. 85, 1342 (1981).

3. C. T. Cheah and M. A. A. Clyne, J. Photochem. 15, 21 (1981).

4. P. D. Whitefield and F. E. Hovis, "Active Nitrogen Generation", Report AFWL-TR-86, McDonnell Douglas Research Laboratories, St. Louis, Missouri (24 March 1986).

Fig. 1. NF(a) Concentrations Calculated for the Conditions of Fig. 8 of Ref. 1 with Values of B = 0.91, 0.6, and 0.3. The calculation is a direct integration of the 4 reaction mechanism of ref. 1. (Note: The value of the recombination rate depends on the value of B).

8

FIGURES FROM REFERENCE 1
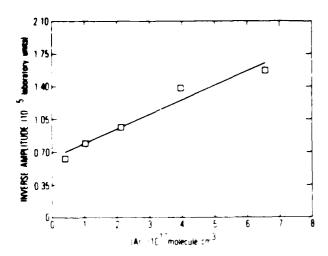
FIG 6 Plot of NF(a) amplitudes vs [Ar] according to Eq. (3). H_2 and NF_2 densities were held fixed at 8.2×10^{13} and 9.0×10^{15} molecule/cm^3, respectively. KrF laser flux was 7.9×10^{15} photons/cm^2 resulting in an initial F atom concentration of 2.1×10^{13} molecule/cm^3. A linear fit is indicated as well
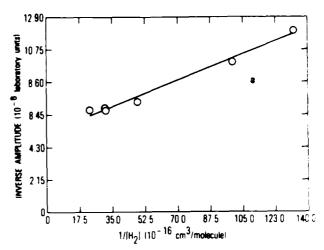
FIG 7. Plot of NF(a) amplitudes vs [H_2] according to Eq. (4). Ar and NF_2 densities were held fixed at 4.0×10^{17} and 9.7×10^{15} molecule/cm^3, respectively. KrF laser flux was 7.9×10^{15} photons/cm^2 resulting in an initial F atom concentration of 2.3×10^{13} molecule/cm^3. A linear fit is indicated as well.
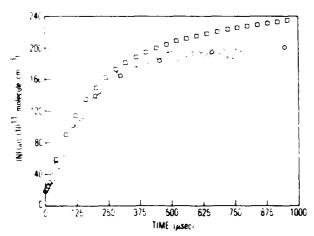

FIG. 8. Formation behavior of NF(a) from KrF photolysis of an $NF_2/H_2/Ar$ mix. The points are the experimental data whereas the squares and circles represent the analytic and NEST model, respectively. Experimental data are scaled to absolute densities using absolute calibration factor (see Sec. III). [Ar] = 4.0×10^{17}, [NF_2] = 9.7×10^{15}, [H_2] = 1.0×10^{14}, [F] = 2.6×10^{13}, [NF(a)] = 2.6×10^{12}, [NF(X)] = 2.3×10^{13}. The slow NF(a) decay rate was included in the NEST model phenomenologically.

10

LABORATORY OPERATIONS

The Aerospace Corporation functions as an "architect-engineer" for national security projects, specializing in advanced military space systems. Providing research support, the corporation's Laboratory Operations conducts experimental and theoretical investigations that focus on the application of scientific and technical advances to such systems. Vital to the success of these investigations is the technical staff's wide-ranging expertise and its ability to stay current with new developments. This expertise is enhanced by a research program aimed at dealing with the many problems associated with rapidly evolving space systems. Contributing their capabilities to the research effort are these individual laboratories:

Aerophysics Laboratory: Launch vehicle and reentry fluid mechanics, heat transfer and flight dynamics; chemical and electric propulsion, propellant chemistry, chemical dynamics, environmental chemistry, trace detection; spacecraft structural mechanics, contamination, thermal and structural control; high temperature thermomechanics, gas kinetics and radiation; cw and pulsed chemical and excimer laser development including chemical kinetics, spectroscopy, optical resonators, beam control, atmospheric propagation, laser effects and countermeasures.

Chemistry and Physics Laboratory: Atmospheric chemical reactions, atmospheric optics, light scattering, state-specific chemical reactions and radiative signatures of missile plumes, sensor out-of-field-of-view rejection, applied laser spectroscopy, laser chemistry, laser optoelectronics, solar cell physics, battery electrochemistry, space vacuum and radiation effects on materials, lubrication and surface phenomena, thermionic emission, photo-sensitive materials and detectors, atomic frequency standards, and environmental chemistry.

Computer Science Laboratory: Program verification, program translation, performance-sensitive system design, distributed architectures for spaceborne computers, fault-tolerant computer systems, artificial intelligence, micro-electronics applications, communication protocols, and computer security.

Electronics Research Laboratory: Microelectronics, solid-state device physics, compound semiconductors, radiation hardening; electro-optics, quantum electronics, solid-state lasers, optical propagation and communications; microwave semiconductor devices, microwave/millimeter wave measurements, diagnostics and radiometry, microwave/millimeter wave thermionic devices; atomic time and frequency standards; antennas, rf systems, electromagnetic propagation phenomena, space communication systems.

Materials Sciences Laboratory: Development of new materials: metals, alloys, ceramics, polymers and their composites, and new forms of carbon; non-destructive evaluation, component failure analysis and reliability; fracture mechanics and stress corrosion; analysis and evaluation of materials at cryogenic and elevated temperatures as well as in space and enemy-induced environments.

Space Sciences Laboratory: Magnetospheric, auroral and cosmic ray physics, wave-particle interactions, magnetospheric plasma waves; atmospheric and ionospheric physics, density and composition of the upper atmosphere, remote sensing using atmospheric radiation; solar physics, infrared astronomy, infrared signature analysis; effects of solar activity, magnetic storms and nuclear explosions on the earth's atmosphere, ionosphere and magnetosphere; effects of electromagnetic and particulate radiations on space systems; space instrumentation.

...

END

FILMED

MARCH, 1988

DTIC